Vortex matter in anisotropic superconductors

Eli Zeldov

Weizmann Institute of Science, Rehovot, Israel

Vortices threading type-II superconductors in presence of magnetic field are remarkable extended particles that interact with each other and with the underlying material disorder forming a substance that is generally referred to as vortex matter [1]. A striking property of vortex matter is that the various energy scales can be readily tuned over a wide range of parameters, thus providing a unique system for investigation of a broad range of fundamental questions in statistical mechanics and condensed matter physics [2]. Since the discovery of high-T_c superconductors (HTS) it has been recognized that the complexity of vortex matter results in a very rich phase diagram and in various unique equilibrium structures much of which are still unresolved [3]. Even less understood is the response of the vortex lattice to applied forces, i.e., the dynamics of vortex matter. It is expected that a moving lattice should display a dynamic phase diagram that is even more intriguing and diverse than the already rich static phase diagram. In addition, the most relevant aspect of superconductors for technological applications – their capability to carry loss-free currents – is determined entirely by vortex dynamics.

Our level of knowledge of vortex matter in superconductors has experienced a revolution in recent years. Because of the elevated temperatures and high anisotropy of HTS, the role of thermal fluctuations are significantly enhanced and the mean-field picture of an ordered solid vortex lattice made of parallel straight vortices that was used in the context of conventional superconductors became vastly insufficient. A multitude of new phenomena were discovered

both experimentally and theoretically, most of them arising from the interplay of the enhanced fluctuations, different types of point and correlated disorder, layered structure of the HTS, symmetry of the order parameter, and surface and geometrical effects. Clearly, it is impossible to provide a meaningful overview of the field in such a limited space. I have therefore chosen to describe three intriguing aspects of the static properties of the vortex matter which I have encountered personally. These phenomena are just a few examples of the new insight that emerged from development of novel experimental tools that provide local information in contrast to the commonly utilized global tools. They provide a historic perspective of the advancement of local measurements and their impact on our current understanding of vortex matter in HTS.

Local magnetization and geometrical barriers

Magnetization is one of the most commonly studied properties of superconductors that provides information on both the static and dynamic behavior of vortices. Of particular interest are the magnetic hysteresis and the irreversibility line on the field-temperature (H-T) diagram that demarcates the hysteretic magnetization behavior at low fields and temperatures from the reversible magnetization above the line. The common source of magnetic hysteresis is vortex pinning due to material disorder, giving rise to a finite critical current below which vortices are immobile. In this case the magnetic hysteresis of a sample is described by the Bean model according to which upon increasing magnetic field vortices gradually penetrate from the sample edges forming steep slopes like sand dunes moving into the sample. The gradient of the vortex density is determined by the critical current with a maximum in vortex density at the edges and minimum in the center. On decreasing magnetic field vortices resemble a sand pile with highest vortex density in the center and lowest near the edges. This mechanism causes magnetic hysteresis which is a convenient contact-less measure of the critical current of a superconductor

that is of central importance for applications.

The magnetic hysteresis is commonly studied by global measurements that determine the total magnetic moment of the sample. In the early 90s we developed with M. Konczykowski arrays of very sensitive microscopic Hall sensors using the two-dimensional electron gas in GaAs. Our early studies of BSCCO crystals revealed a very surprising phenomenon in which vortices seemed to "appear" mysteriously in the center of the sample forming a vortex puddle with a dome shaped density surrounded by a vortex free region [4]. With increasing field the dome grew from the sample center outwards. Similar observations were obtained using magneto-optical imaging [5]. These puzzling findings were counterintuitive in view of the Bean model according to which a vortex front should gradually penetrate from the edges towards the center upon increasing the field. Having studied extensively the expected current and field distributions in platelet samples in perpendicular fields within the Bean model with John Clem [6], we soon gained the following qualitative understanding of the phenomenon. Bulk pinning in the anisotropic HTS is very weak at elevated temperatures and therefore one would expect a reversible magnetization in a bulk sample. The situation, however, is very different in a thin sample in perpendicular field. If the sample has an elliptical cross-section it can be shown that the magnetic induction B inside the sample will be uniform at any applied field. This result can be understood as follows. A test vortex that resides inside the sample experiences two forces. The first force arises from the fact that in an elliptical sample the length of the vortex and hence its total line energy is position dependent which results in an outward force that is proportional to the derivative of the vortex elongation. The second force is due to the Meissner shielding currents that circulate along the surface and push the vortex towards the sample center. It turns out that for an elliptical shape these

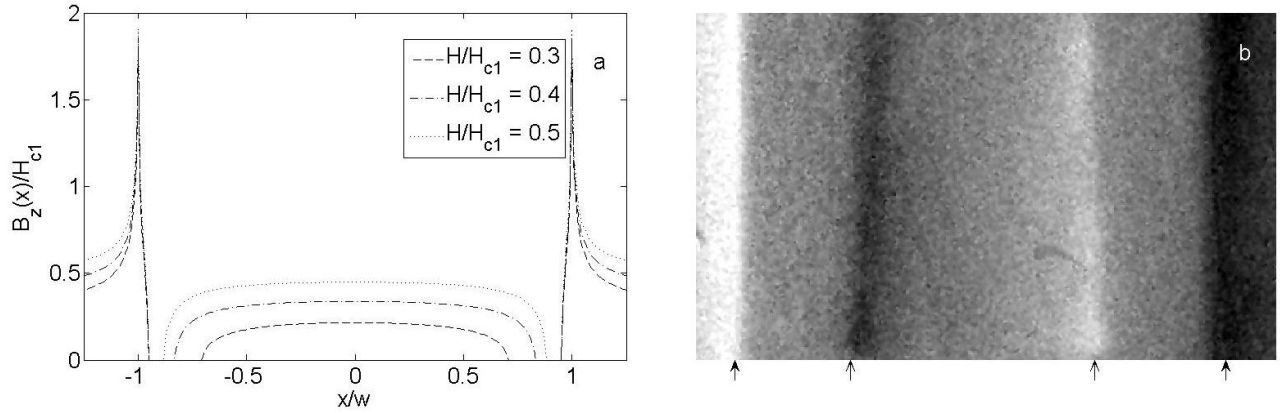

Fig. 1. (a) Calculated field profile $B_z(x)$ across the width –W<x<W of an infinitely long superconducting strip of thickness d (d/W=0.1) for three values of increasing applied field H. The vortex dome in the center of the sample is the result of a geometrical barrier and it grows with increasing H. (b) Differential magneto-optical image of a segment of a long BSCCO crystal strip at H = 6.8 Oe and T = 75 K, showing the vortex dome between the inner arrows [7]. The outer arrows mark the edges of the crystal of width 2W = 420 μm. The differential image is obtained by subtracting images with positive and negative periodic transport current of 10 mA applied along the strip. The bright and dark shades of the dome edges result from the differential imaging of the small periodic right and left shift of the dome caused by the applied current.

two forces cancel out exactly resulting in a position independent vortex energy and hence in a constant B throughout the sample. In platelet crystals with rectangular cross-section the first force is absent and thus the vortices that penetrate through the edges are rapidly driven towards the center forming a dome shaped vortex puddle as shown in Figure 1a. This dome grows as the applied field is increased giving the impression that the vortices appear in the sample center and expand outwards.

Having some understanding of the underplaying mechanism, our next challenge was to find a proper solution. In the early 1990s, the Physics Department at the Weizmann Institute has established a special program which hosted a large group of leading Soviet physicists from the

Landau Institute for an extended period of time. I discussed this puzzle with Anatoly I. Larkin and his former student Dima Geshkenbein, who were part of the Landau-Weizmann program. In the first couple of meetings, which we had to conduct with my very limited Russian at that time, most of the interaction was with Dima, while Anatoly Ivanovich was observing quietly. Then, in a following meeting Anatoly all of a sudden started to talk and right away came up with an ingenious insight: since the currents are present in the vortex free regions and there is no current in the vortex filled region, *B* and *J* are mutually exclusive, and hence they have to be the imaginary and real parts of a complex function. He then immediately guessed that this complex function has to be of the form $\sqrt{(b^2 - x^2)/(W^2 - x^2)}$, where *b* is the half-width of the dome and *W* the half-width of the sample. By proper integration of this trial function I was amazed to find out that Larkin's guess was an exact solution and fully described the current and field distributions. This vivid encounter with Larkin's genius left an extraordinary impression on me. We coined the phenomenon geometrical barrier, since the vortices have to overcome an extended potential barrier of geometrical origin, and expanded this approach to take a proper account of sample edges and of bulk pinning [4]. Figure 1a shows the calculated field profiles $B_z(x)$ at various values of increasing applied field including a more detailed treatment of the sample edges in absence of bulk pinning.

Figure 1b shows an experimental manifestation of the geometrical barrier and of the vortex dome in a BSCCO crystal using differential magneto-optical imaging [7]. The vortices in the dome are trapped by the Meissner currents and cannot leave the sample. Upon decreasing the field the dome expands while preserving the total flux trapped in it. Vortices can leave the sample only when the edges of the dome reach the sample edges. As a result, the geometrical barrier gives rise to magnetic hysteresis even in the absence of any bulk pinning. Vortex penetration starts at

field $H_p \approx H_{c1}\sqrt{d/W}$ and the hysteresis persists up to fields of the order of H_{c1}. The effect of the geometrical barrier can be further significantly enhanced if a Bean-Livingston surface barrier is also present giving rise to a combined edge barrier that can persist to much higher fields [8,9].

Vortex lattice melting

Following the discovery of HTS an extensive discussion of the possible melting of the vortex lattice emerged. In the context of conventional low T_c SC this question was of no real significance since the melting should occur essentially at the disappearance of superconductivity at H_{c2}. In HTS, in contrast, theoretical studies suggested that the highly enhanced thermal fluctuations may lead to melting of the lattice well below H_{c2} [2,3,10]. In addition to the great scientific interest, this possibility had a major practical implication, since the vortex liquid cannot support any critical current. It was predicted that in disordered systems the melting may occur through a second order transition, whereas in clean systems with an ordered lattice the melting should occur through a first-order phase transition (FOT) [1-3,10-13]. The issue became a vigorously debated topic with numerous controversial experimental studies. Neutron scattering experiments showed disappearance of Bragg peaks [14], which indicated loss of long range order of the lattice, and transport measurements in YBCO singe crystals revealed a sharp drop in resistivity consistent with freezing of the lattice [15,16]. None of the experiments, however, provided a thermodynamic signature of a FOT.

All the initial searches for the melting transition were based on global measurements. It turned out that having local information was essential for the detection of the FOT. At that time we used arrays of Hall sensors to investigate the so-called second magnetization peak in BSCCO crystals

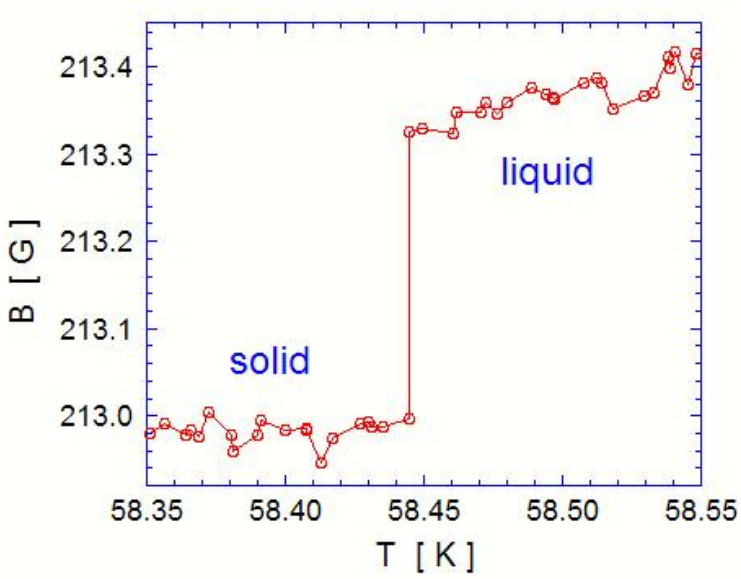

Fig. 2. Discontinuous step in the local vortex density and induction *B* across a first-order melting transition in a BSCCO crystal. The data were measured by an array of 10x10 μm^2 Hall sensors on sweeping temperature at a constant applied field of 240 Oe [20]. The transition occurs at slightly different temperature at the location of each sensor. The vortex density in the liquid is higher than in the solid. Vortex liquid thus behaves like water that expands upon freezing into ice when cooled at a constant pressure.

[17]. This large peak in hysteretic magnetization is visible at low temperatures at which the critical current of the sample appears to increase at some characteristic field B_{sp} that is almost temperature independent. With increasing temperature the peak shrinks and seems to disappear at some intermediate temperature. We noticed that at higher temperatures a small step appeared in the data in place of the second magnetization peak. This step was hardly visible but seemed to be reproducible and hence we decided to study it more carefully. We were very fortunate to have very high quality BSCCO crystals grown by N. Motohira in the lab of K. Kishio and K. Kitazawa in University of Tokyo [18], which turned out to be the cleanest and most uniform crystals I have ever encountered. We improved the sensitivity of our Hall probes and carried out measurements of the local induction *B* using very dense temperature and field sweeps. A small

but an extremely sharp step ΔB became evident, see Figure 2, the location of which traced a well defined $B_m(T)$ line on the H-T phase diagram extending from the region of the second magnetization peak to T_c. Moreover, this step occurred at slightly different field or temperature at different places across the sample as revealed by the different Hall sensors in the array. We had numerous debates of this step with Geshkenbein, Larkin, and Vinokur considering its different possible origins. Shortly prior to a workshop organized by M. Konczykowski in the Ecole Polytechnique in 1994, a paper by the group of Paco de la Cruz had been published [19] which showed evidence of such a step in global magnetization measurements at high temperatures and was interpreted as a FOT of the lattice. Following further exciting discussions at the workshop, I became convinced that the sharp step that we observed is a direct thermodynamic observation of the first-order melting of the vortex lattice [20]. Locally this transition is very sharp, however, at each location it occurs at a somewhat different field or temperature due to disorder and geometrical barriers, and therefore is very hard to be detected by global magnetization measurements. In YBCO crystals the melting transition extends to much higher fields due to the lower anisotropy, and therefore the broadening of the transition is relatively smaller. As a result, subsequent high sensitivity studies of magnetization and specific heat succeeded to resolve the FOT also in YBCO crystals by global measurements [21,22].

The arrays of Hall probes showed that there is a nontrivial coexistence of the solid and liquid phases in the sample over a wide range of fields and temperatures. We therefore were very interested in visualization of this melting process on a microscopic scale. For this purpose we developed differential magneto-optical (DMO) imaging [23]. In conventional magneto-optics (MO) typical sensitivity is of the order of a few Gauss which is insufficient to distinguish the difference in the induction between the solid and liquid phases ΔB that is typically of the order of

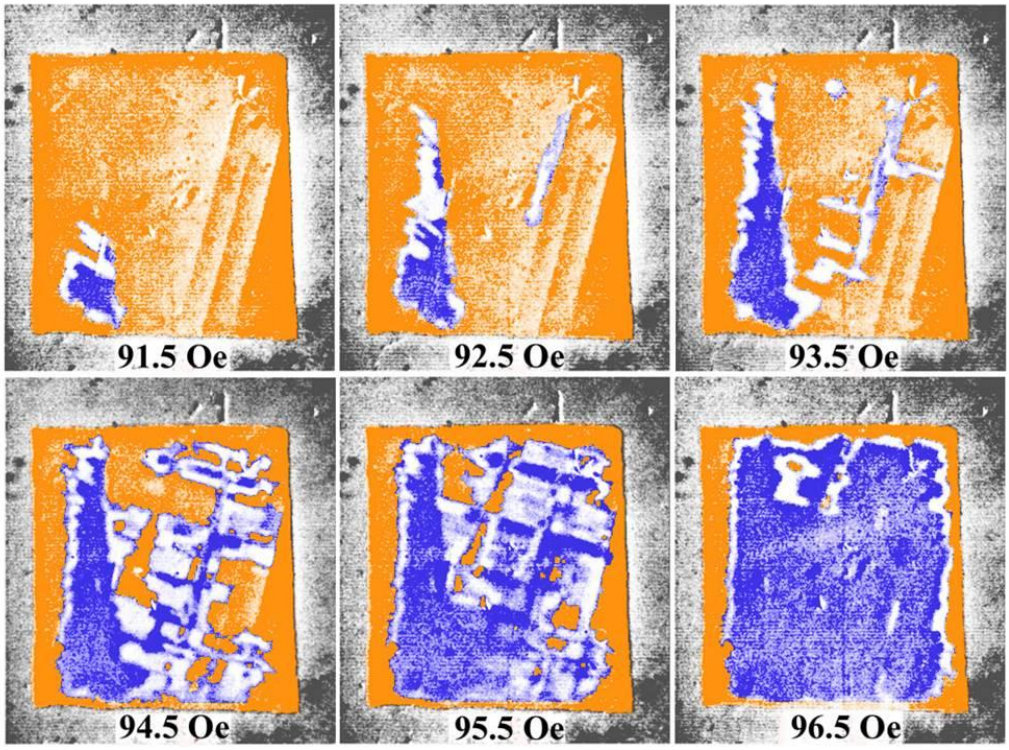

Fig. 3. Vortex lattice melting process in BSCCO crystal of 1.1x1.2 mm^2 as revealed by differential magneto-optical imaging upon increasing field at constant T= 70 K [23]. At low fields the entire crystal is in the solid phase (brown). At 91.5 Oe an irregular liquid droplet (blue) is formed in the lower left corner. On the right hand side three parallel defects are visible along one of the crystallographic directions. With increasing field complicated melting patterns are obtained with numerous solid and liquid domains that have preferential orientation either parallel or perpendicular to the crystallographic directions. At 96.5 Oe a large liquid region is present in the center, with a few solid islands in the top part. The presence of the liquid phase in the sample center surrounded by vortex solid is the result of the geometrical-barrier vortex dome profile. The full movie is available at http://www.weizmann.ac.il/condmat/superc/.

0.1 G. The sensitivity of the MO is mainly limited by the inhomogeneities in the MO indicators and the shot noise in the CCD cameras. Both these limitations can be levitated by periodically modulating either the applied field by a small δH or the temperature by δT and averaging over many corresponding differential images. If vortex solid and liquid regions coexist in the sample, increasing the temperature by a small δT will slightly expand the liquid domains. In the regions

where the solid-liquid interface has shifted the local induction increases by ΔB while essentially no change occurs in the rest of the sample. As a result the solid-liquid interface in DMO image will appear bright as shown in Figure 3. By taking a series of DMO images as a function of temperature or field a movie of the entire melting process is thus obtained [23]. We found that the quenched material disorder results in a complicated melting temperature T_m landscape [24] that causes formation of intricate melting patterns and coexistence of solid and liquid domains as exemplified in Figure 3. As a result the sharp local FOT becomes significantly broadened and hard to be resolve in global measurements.

Vortex matter phase diagram

The discovery of the FOT established that the vortex matter in HTS displays at least two thermodynamic phases. Additional studies showed that the phase below the transition has a finite shear modulus and some degree of long range order as reflected by the Bragg peaks in neutron scattering and magnetic decoration experiments, and therefore is a vortex solid. According to Larkin and Ovchinikov, however, quenched disorder should always destroy the long-range order of the lattice [25]. A conceptual breakthrough was obtained when the theory of Bragg glass was developed [26,27], according to which dislocations are not formed at sufficiently weak disorder and as a result the lattice displays algebraic quasi-long-range translational order. This theory was consistent with the experimental observation of Bragg peaks and the existence of first-order melting, at which dislocations proliferate causing loss of order. In weakly anisotropic HTS like YBCO the liquid phase is believed to constitute a highly entangled state of vortex lines dominated by thermal fluctuations. In materials with high anisotropy, like BSCCO, there is experimental evidence for simultaneous melting and decoupling at the FOT, namely in the high

temperature phase the vortex lines decompose into a gas-like state of uncorrelated vortex pancakes in the individual CuO_2 planes [28].

This understanding, however, applied only to the high temperature part of the vortex matter phase diagram. The experimental difficulty is that at low temperatures vortex matter is dominated by strong pinning due to quenched disorder. As a result, the vortex matter is usually far away from the equilibrium state and magnetization measurements show highly hysteretic behavior which completely masks the thermodynamic properties of the lattice. Consequently the FOT was found to terminate at some intermediate temperatures [20]. The resolution to this experimental limitation came with the introduction of vortex shaking by an in-plane ac field that was originally applied to YBCO crystals at high temperatures [29,30]. We found that in highly anisotropic materials like BSCCO vortex shaking is very effective in equilibrating the vortex lattice at low temperatures, thus opening a new avenue for the investigation of the thermodynamic phase diagram in regions that were previously inaccessible [31]. The addition of an in-plane field in highly anisotropic HTS results in the formation of crossing lattices in which stacks of pancake vortices (PVs) coexists with a lattice of Josephson vortices (JVs) that reside in-between the CuO_2 planes [32]. The JVs are weakly pinned and therefore remain highly mobile even at low temperatures. An in-plane ac field thus results in a periodic motion of JVs that repeatedly intersect the stacks of PVs at random places. The circulating currents of the JVs exert a local force on the PVs at the intersections, thus causing a random local shaking of the PVs that results in a gradual equilibration of the vortex lattice.

By combining local magnetization measurements with vortex shaking, we discovered that the FOT extends to much lower temperatures and traces the location of the second magnetization peak. Moreover, in this region the vortex matter displays a unique phenomenon of inverse

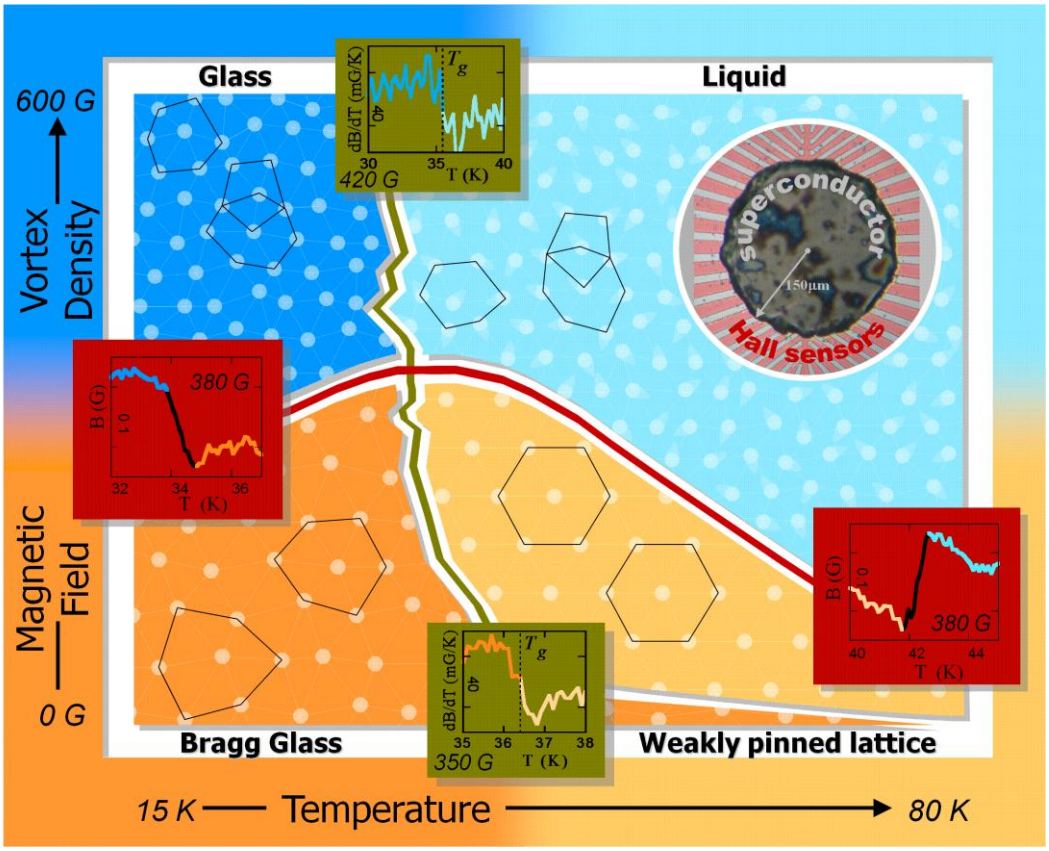

Fig. 4. Schematic vortex matter phase diagram in BSCCO as revealed by local magnetization measurements in presence of vortex shaking by in-plane ac field [33]. Four thermodynamic phases are suggested to be formed by two intersecting phase transition lines. The red line is a single first-order transition $B_m(T)$ that gradually changes its character from thermally-driven melting at high temperatures to disorder-driven transition displaying an inverse melting behavior at low temperatures. A positive step ΔB in the local induction occurs upon increasing temperature across the thermal meting (right inset) and a negative step across the inverse melting (left inset). The green line is apparently a second-order transition T_g characterized by a step-like change in the slope dB/dT (top and bottom insets). The top-right phase is vortex liquid that undergoes a glass transition into a glassy phase upon decreasing temperature. The two blue phases are entangled with high concentration of dislocations. The two brown phases are vortex solid with no dislocations. The low-temperature phase is apparently strongly pinned Bragg glass. The high-temperature region is weakly pinned and may display a higher extent of order. The top-right inset shows a disk-shaped BSCCO crystal residing on an array of microscopic Hall sensors.

melting in which the lattice crystallizes upon increasing rather than decreasing temperature [31,33]. The red curve in Figure 4 shows the full FOT line $B_m(T)$ in BSCCO which displays a maximum at intermediate temperatures followed by a change of slope in the inverse melting region. At high temperatures the solid vortex lattice is destroyed by thermal fluctuations, whereas at low temperatures the lattice is destroyed by pinning due to quenched disorder which becomes dominant over the elastic energy as the field is increased [34]. As a result, the lattice transforms into an amorphous entangled state with a high concentration of dislocations. The FOT is thus a single line that gradually changes its character from predominantly thermally driven melting to predominantly point disorder driven transition [35]. The inverse melting behavior results from the fact that with increasing temperature the vortex pinning is reduced by thermal fluctuations resulting in an increasing $B_m(T)$ [36-38].

By increasing the temperature at intermediate fields, the FOT line can be crossed twice. In this interesting case, a negative ΔB step is observed on the first crossing in the inverse melting part (left inset in Figure 4), followed by a positive ΔB step in the region of thermally driven FOT (right inset). Moreover, in-between the two FOT steps, we found a sharp kink in B(T) which indicates a possible existence of a second-order transition (SOT) line as shown by the green curve in Figure 4. Along this line a sharp change in the slope dB/dT is revealed in local measurements in regions both below and above the FOT as shown by the top and bottom insets [33]. The existence of a SOT at elevated fields implies that instead of a single vortex liquid phase above the FOT line, two distinct phases are present – a vortex liquid and glassy phase separated by a glass transition line. The continuation of the SOT line into the vortex solid region below the FOT line, however, is much more surprising. This entire region of the phase diagram is believed to be the Bragg glass phase [3,27,38]. The existence of the SOT line implies that this region is

subdivided into two distinct thermodynamic phases [39]. The low-temperature phase displays strong pinning and hence is presumably the Bragg glass phase. In the high-temperature part the pinning is extremely weak due to enhanced thermal fluctuations which could lead to a solid phase with partially recovered long-range order. The presented diagram with the proposed four thermodynamic phases, calls for new experimental and theoretical studies in order to comprehend the evermore intriguing nature of vortex matter in high-temperature superconductors.

References

1. M. Tinkham, *Introduction to Superconductivity* (Mc Graw Hill, New York, 1996).
2. G. Blatter, M. V. Feigelman, V. B. Geshkenbein, A. I. Larkin, V. M. Vinokur, Rev. Mod. Phys. **66** (1994) 1125
3. T. Giamarchi and S. Bhattacharya, *High Magnetic Fields: Applications in Condensed Matter Physics, Spectroscopy* (Springer, 2002), p. 314.
4. E. Zeldov, A. I. Larkin, V. B. Geshkenbein, M. Konczykowski, D. Majer, B. Khaykovich, V. M. Vinokur, and H. Shtrikman, Phys. Rev. Lett. **73** (1994) 1428
5. M.V. Indenbom, H. Kronmüller, T.W. Li, P.H. Kes and A.A. Menovsky, Physica C **222** (1994) 203
6. E. Zeldov, J. R. Clem, M. McElfresh, and M. Darwin, Phys. Rev. B **49** (1994) 9802
7. Y. Segev, I. Gutman, S. Goldberg, Y. Myasoedov, E. Zeldov, E. H. Brandt, G. P. Mikitik, and T. Sasagawa, unpublished.
8. E. H. Brandt, Phys. Rev. B **60** (1999) 11939
9. J. Clem, Journal of Superconductivity and Novel Magnetism **21** (2008) 343
10. D. R. Nelson, Phys. Rev. Lett. **60** (1988) 1973

11. M. P. A. Fisher, Phys. Rev. Lett. **62** (1989) 1415
12. E. H. Brandt, Rep. Prog. Phys. **58** (1995) 1465
13. T. Nattermann and S. Scheidl, Adv. Phys. **49** (2000) 607
14. R. Cubitt, E. M. Forgan, G. Yang, S. L. Lee, D. McK. Paul, H. A. Mook, M. Yethiraj, P. H. Kes, T. W. Li, A. A. Menovsky, Z. Tarnawski, and K. Mortensen, Nature **365** (1993) 407
15. H. Safar, P. L. Gammel, D. A. Huse, D. J. Bishop, J. P. Rice, and D. M. Ginsberg, Phys. Rev. Lett. **69** (1992) 824
16. W. K. Kwok, S. Fleshler, U. Welp, V. M. Vinokur, J. Downey, G. W. Crabtree, and M. M. Miller, Phys. Rev. Lett. **69** (1992) 3370
17. B. Khaykovich, E. Zeldov, D. Majer, T. W. Li, P. H. Kes, and M. Konczykowski, Phys. Rev. Lett. **76** (1996) 2555
18. N. Motohira, K. Kuwahara, T. Hasegawa, K. Kishio, and K. Kitazawa, J. Ceram. Soc. Jpn. Int. Ed. **97** (1989) 994
19. H. Pastoriza, M. F. Goffman, A. Arribére, and F. de la Cruz, Phys. Rev. Lett. **72** (1994) 2951
20. E. Zeldov, D. Majer, M. Konczykowski, V. B. Geshkenbein, V. M. Vinokur, and H. Shtrikman, Nature **375** (1995) 373
21. U. Welp, J. A. Fendrich, W. K. Kwok, G. W. Crabtree, and B. W. Veal, Phys. Rev. Lett. **7** (1996) 4809
22. A. Schilling, R. A. Fisher, N. E. Phillips, U. Welp, D. Dasgupta, W. K. Kwok, G. W. Crabtree, Nature **382** (1996) 791
23. A. Soibel, E. Zeldov, M. Rappaport, Y. Myasoedov, T. Tamegai, S. Ooi, M. Konczykowski, and V. B. Geshkenbein, Nature **406** (2000) 282
24. A. Soibel, Y. Myasoedov, M. L. Rappaport, T. Tamegai, S. S. Banerjee, and E. Zeldov, Phys.

Rev. Lett. **87** (2001) 167001

25. A. I. Larkin and Y. N. Ovchinnikov, J. Low Temp. Phys **34** (1979) 409
26. T. Nattermann, Phys. Rev. Lett. **64** (1990) 2454
27. T. Giamarchi and P. Le Doussal, Phys. Rev. Lett. **72** (1994) 1530
28. D. T. Fuchs, R. A. Doyle, E. Zeldov, D. Majer, W. S. Seow, T. Tamegai, S. Ooi, R. Drost, M. Konczykowski, and P. H. Kes, Phys. Rev. B **55** (1997) R6156
29. M. Willemin, A. Schilling, H. Keller, C. Rossel, J. Hofer, U. Welp, W. K. Kwok, R.J. Olsson, and G. W. Crabtree, Phys. Rev. Lett. **81** (1998) 4236
30. E. H. Brandt and G. P. Mikitik, Phys. Rev. Lett. **89** (2002) 027002
31. N. Avraham, B. Khaykovich, Y. Myasoedov, M. Rappaport, H. Shtrikman, D. E. Feldman, T. Tamegai, P. H. Kes, M. Li, M. Konczykowski, K. van der Beek, and E. Zeldov, Nature **411** (2001) 451
32. A. E. Koshelev, Phys. Rev. Lett. **83** (1999) 187
33. H. Beidenkopf, N. Avraham, Y. Myasoedov, H. Shtrikman, E. Zeldov, B. Rosenstein, E. H. Brandt, and T. Tamegai, Phys. Rev. Lett. **95** (2005) 257004
34. V. Vinokur, B. Khaykovich, E. Zeldov, M. Konczykowski, R. A. Doyle, and P. H. Kes, Physica C **295** (1998) 209
35. P. Olsson and S. Teitel, Phys. Rev. Lett. **87** (2001) 137001
36. D. Ertas and D. R. Nelson, Physica C **79** (1996) 272
37. H. Beidenkopf, T. Verdene, Y. Myasoedov, H. Shtrikman, E. Zeldov, B. Rosenstein, D. Li, and T. Tamegai, Phys. Rev. Lett. **98** (2007) 167004
38. G. P. Mikitik and E. H. Brandt, Phys. Rev. B **68** (2003) 054509
39. D. Li, B. Rosenstein, and V. Vinokur, J. Superconductivity and Novel Magnetism **19** (2006) 369